Journal of the Korean Ceramic Society
Vol. 55, No. 1, pp. 80~84, 2018.

https://doi.org/10.4191/kcers.2018.55.1.01

The Influence of Functionalization of the Fe_3O_4 Nanoparticle on its Dispersion Property

Jin Soon Han*, Gye Seok An*,, Bong Geun Park*, and Sung-Churl Choi*,†**

**Division of Materials Science & Engineering, Hanyang University, Seoul 04763, Korea*
***Engineering Ceramic Center, Korea Institute of Ceramic Engineering and Technology, Icheon 17303, Korea*

(Received November 8, 2017; Revised November 10, 2017; Accepted November 13, 2017)

ABSTRACT

In this study, to improve the dispersity of Fe_3O_4 nanoparticles, dispersion properties were considered with various types of functionalization of Fe_3O_4 nanoparticles. Due to its high surface area, the electrically neutral state of its surfaces, and its magnetic momentum, Fe_3O_4 nanoparticles are easily aggregated in solution. In order to prevent aggregation, Fe_3O_4 nanoparticles were functionalized with carboxyl and amine groups in the form of a polymer compound. Carboxyl and amine groups were attached to the surface of Fe_3O_4 nanoparticles and the absolute value of the zeta potential was found to be enhanced by nearly 40 eV. Furthermore, the morphology and the magnetic property were analyzed for the application of Fe_3O_4 nanoparticles as a magnetic fluid.

Key words : Fe_3O_4, Magnetic nanoparticle, Functionalization, Zeta potential, Dispersion

1. Introduction

The properties that a magnetic material has have, with the development of the relevant technologies, been applied to various industrial fields, ranging from electronics to arts and medical care.[1,2] In particular, the high saturation magnetization value and coercive force, which are superparamagnetic properties that are expressed when ferromagnetic substances are downsized to nanoparticles, and the absence of a residual magnetization value,[3] have been applied to various fields including magnetic fluid-based nonferrous metal separation, focusing on convenience in the control of nanoparticles.[2,4,5] The difficulties involved in particle recovery that are caused by the high dispersive force required by conventional nanoparticles, as well as the small particle size, may be overcome by applying a magnetic attractive force generated by an external magnetic field, which allows for rapid recovery of the particles. This finding has been applied to drug delivery systems, DNA separation and purification, and magnetic resonance imaging (MRI) to enable targeting or rapid recovery.[5-7] Studies have been conducted on superparamagnetic properties that enable not only rapid recovery of superparamagnetic nanoparticles but also re-dispersion of the recovered particles, as well as on particle aggregation control using the high saturation magnetization value.[8,9] However, in the absence of an external magnetic field, despite the absence of a residual magnetization value, the magnetic moment for the expression of the magnetic properties still affects the surroundings, resulting in the generation of a local attractive force. Therefore, after particle recovery by means of an external magnetic field, some particles may not be re-dispersed and overall aggregation of the particles may occur in the absence of an external magnetic field, imparting a negative effect on the particle dispersibility.

Such exacerbation of the dispersibility impedes the realization of uniform nanoparticle properties and decreases the surface characteristics. In addition, in the functionalization of superparamagnetic nanoparticles through the introduction of an amphiphilic material to the surfaces, formation of a coating layer on individual particles becomes difficult due to the formation of core-shell type particles.[10] The coating layer formed on the aggregated particles spoils the advantage of the nanoparticles, the high specific surface area, and thus reduces the overall efficiency of the functional groups. Many studies have been conducted to solve this problem.[8,11] In previous studies, efforts have been made to improve the dispersibility by focusing on steric hindrance and electrostatic hindrance, which are the major mechanisms of dispersion. With regard to steric hindrance, studies have been conducted to hinder the physical contact between particles by forming a bilayer or by attaching an amphiphilic material.[6,12] Due to the hydrophobicity of Fe_3O_4 superparamagnetic nanoparticles, these attempts to hinder physical contact have been realized by using an organic solvent and an organic dispersing agent, which may cause environmental pollution and which have limitations in application because of low biocompatibility. With regard to electrostatic hindrance, experiments have been conducted for the surface treatment of Fe_3O_4 nanoparticles using an acidic or basic

†Corresponding author : Sung-Churl Choi
E-mail : choi0505@hanyang.ac.kr
Tel : +82-2-2220-0505 Fax : +82-2-2291-6767

solution and for the formation of hydroxyl groups on the surface through the formation of an SiO_2 layer.[8,12] These experiments have shown that the surface modification of superparamagnetic nanoparticles may improve the dispersibility. The negative charges existing in the hydroxyl groups may provide a dispersion environment in an aqueous solution, which may enable more environment-friendly preparation of superparamagnetic nanoparticle dispersion solutions that may be used for various purposes. Studies have been carried out to investigate how the dispersion of superparamagnetic nanoparticles is affected by the introduction of amine groups and carboxyl groups, which are representative functional groups having both positive and negative charges.

The purpose of the present study is to establish an environment showing more appropriate dispersion properties based on the electrostatic effects achieved by the surface modification of Fe_3O_4 superparamagnetic nanoparticles with positive and negative charges. Nanoparticles having surfaces functionalized with carboxyl groups and amine groups were successfully prepared by modifying the surfaces using polymer compounds having functional groups. The dispersibility of the particles improved using the positive and negative charges was evaluated and discussed.

2. Experimental Procedures

2.1. Synthesis of Fe_3O_4 nanoparticles

Clustered Fe_3O_4 nanoparticles were prepared by the polyol method. First, 0.4 M of iron (III) chloride hexahydrate ($FeCl_3 \cdot 6H_2O$; 99%, Daejung Chemicals & Materials Co., Korea), the Fe precursor, was dissolved in 100 ml of distilled water, and 0.05 M sodium acetate (> 98.5%, Samchun Pure Chemical Co., Korea) was added to the resulting solution and completely dissolved. Then, the resulting suspension was added to 100 ml of ethylene glycol (EG; 99%, Daejung Chemicals & Materials Co., Korea), and the mixture was heated and refluxed at 150°C for 24 h. After the completion of the reaction, the powder produced was purified from the suspension using a 5000 gauss magnet. The residual organic and inorganic byproducts were removed from the purified powder by performing ultrasonic washing several times using a mixture of distilled water and ethanol (50:50).

2.2. Surface treatment of Fe_3O_4 nanoparticles with polymer compounds

The prepared cluster-shaped Fe_3O_4, with a weight of 0.1 g, was re-dispersed in 100 ml of distilled water through sonication. The dispersion solution was poured into a 500 ml three-neck round bottle flack (RBF) and stirred at 300 rpm for about 30 minutes. Then, either 0.3 g of polyacrylic acid (PAA, Mw 26,000, Sigma-Aldrich, USA) or 0.25 g of polyethylenimine (PEI, Mw, 25,000 branched, Sigma-Aldrich, USA) was added. Subsequently, while stirring at 300 rpm, the solution was heated at 60°C for about 24 h and then cooled naturally. After the completion of the reaction, the suspension was purified using a 5000 gauss magnet. The residual organic and inorganic byproducts were removed from the purified powder by performing ultrasonic washing several times using 200 ml of distilled water.

2.3. Evaluation of properties

The surface functional groups of the recovered product were analyzed using FT-IR (IRAffinity-1S, Shimadzu, Japan). The particle size distribution and the zeta potential were measured (Zetasizer Nano ZS, Malvern, UK) to evaluate the dispersion and the electrostatic dispersibility of the individual samples. The shape of the particles was analyzed by high-resolution transmission electron microscopy (HRTEM; Tecnai G2 F30 S-Twin, FEI, USA). The magnetic properties of the individual samples were measured in the presence of an external magnetic field ranging from −10 to 10 kOe by using a vibrating-sample magnetometer (VSM; Lake Share 7400, USA).

3. Result and Discussion

Figure 1 shows the FT-IR spectra of the Fe_3O_4 particles, the Fe_3O_4 particles surface-treated using PEI, and the Fe_3O_4 particles surface-treated using PAA. An Fe-O peak at 540 cm^{-1} was commonly found in all the three samples. A C-H peak was found in the range of 1350 to 1480 cm^{-1} in the Fe_3O_4 particles surface-treated using PEI and PAA because of the carbon chains included in PEI and PAA. The amine group included in PEI resulted in an N-H peak found at 1650 cm^{-1}. The sample treated with PAA showed a similar peak from 1670 to 1820 cm^{-1}; this is a peak representing the C=O bond existing in the carboxyl groups. Other peaks found at 3000 to 3600 cm^{-1} in the FT-IR spectra of the two samples that underwent surface modification are peaks caused by water, mostly representing the O-H groups. However, the peak generated by the stretching of the N-H bond was found to be stronger in the PEI-treated sample, where the N-H peak was merged with the O-H peak, than that in the PAA-treated sample.[12] These results show that func-

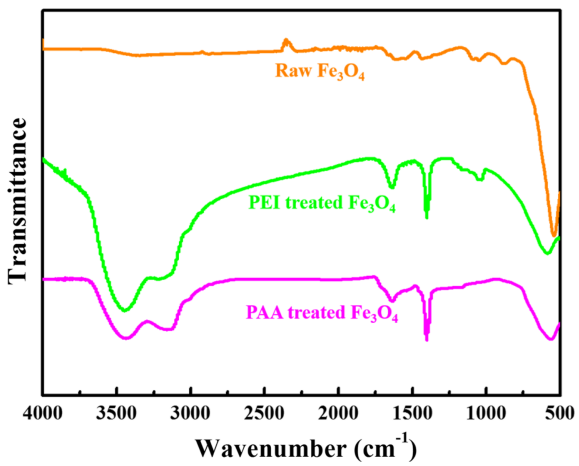

Fig. 1. FT-IR spectra of Fe_3O_4 specimens.

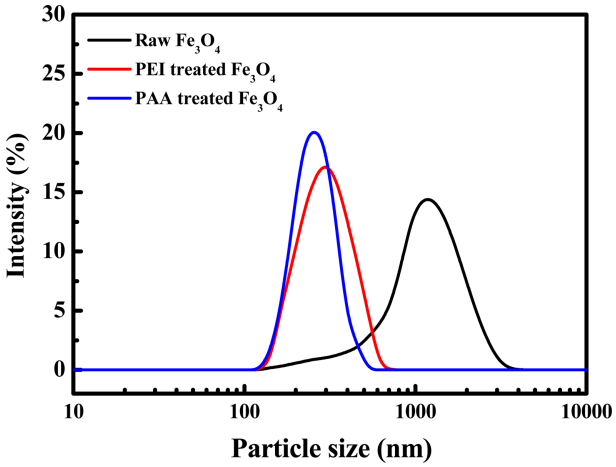

Fig. 2. Particle size distribution of Fe_3O_4 specimens.

tional groups that were not originally on the surface of the Fe_3O_4 particles were formed, modifying the surface properties.

The size distribution of the Fe_3O_4 particles (Fig. 2) treated with each of the polymer compounds was measured. The raw Fe_3O_4 particles showed the largest mean particle size and the widest particle size distribution. The particle size distribution curves of the particles treated with PEI and PAA were shifted to the left, and the size distribution was narrower in comparison with that of the raw Fe_3O_4 particles. The particle size distribution of the raw Fe_3O_4 particles was in a range from 500 to 4000 nm, but changed to a range of 130 to 700 nm through PEI treatment or to a range from 130 to 500 mm through PAA treatment. The particle size distribution was narrower in the PAA-treated particles than in the PEI-treated particles. The mean particle size is about 1327 nm for the raw Fe_3O_4 particles, 308 nm for the PEI-treated particles, and 263 nm for the PAA-treated particles. The polydispersity index was 0.792 for the raw Fe_3O_4 particles, 0.427 for the PEI-treated particles, and 0.214 for the PAA-treated particles. This indicates that the overall particle size decreased as the aggregated raw Fe_3O_4 particles were dispersed. The absolute value of the surface charge (zeta potential), which may be the driving force of dispersion, was 4 eV in the raw Fe_3O_4 particles, but it increased by about 10 times to 37 and 40.3 eV for the PEI-treated and PAA-treated particles, respectively. Assuming that dispersion occurs at a surface charge higher than 20 eV, the dispersibility of the particles may have been improved by the surface treatment with PEI and PAA.[12,13]

Figure 3 provides TEM images of the individual Fe_3O_4 particle samples. The raw Fe_3O_4 particles were found to be almost spherical, with a diameter of about 200 nm. The particles had an uneven surface because they were clusters consisting of smaller nanoparticles. The PEI-treated particles included a thin layer on the surface, which relieved the unevenness of the surface, but the overall particle shape was not significantly different from that of the raw particles. On the contrary, the PAA-treated particles included damage on the particle surfaces. The damage was not so significant that the overall spherical shape could collapse, but the smaller nanoparticles included in the clusters were damaged and showed outstanding surface unevenness. This damage penetrated to the inside, which was verified by the brighter internal regions of the particles. However, although the particles treated with PEI and PAA were damaged on the surface and on the inside, the overall particle shape did not change so much that the cluster shape could

Table 1. Dispersion Properties of Fe_3O_4 Samples

	Raw Fe_3O_4	PEI-treated Fe_3O_4	PAA-treated Fe_3O_4
Mean size (nm)	1327.6	308.3	263.3
Polydispersity index	0.792	0.427	0.214
|Zeta potential| (eV)	4	37	40.3

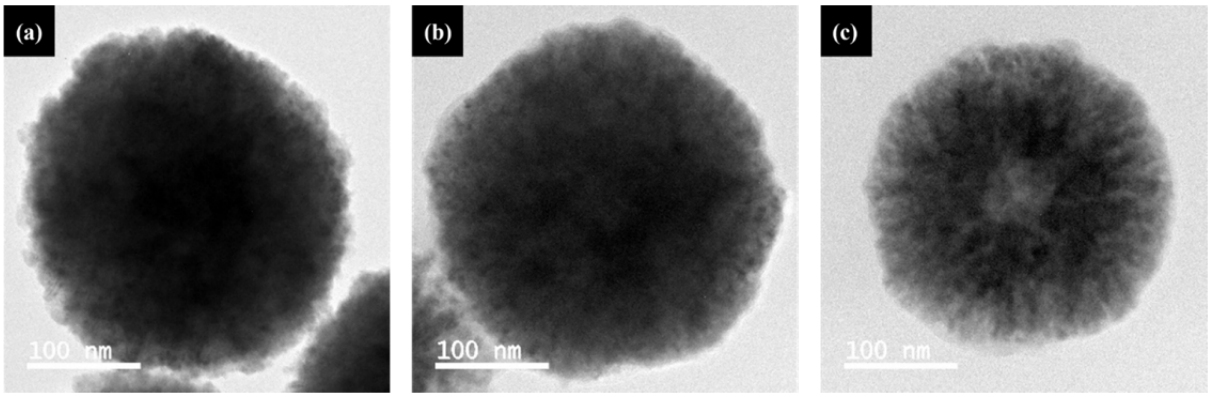

Fig. 3. TEM images of Fe_3O_4 specimens: (a) raw Fe_3O_4, (b) PEI treated Fe_3O_4, (c) PAA treated Fe_3O_4.

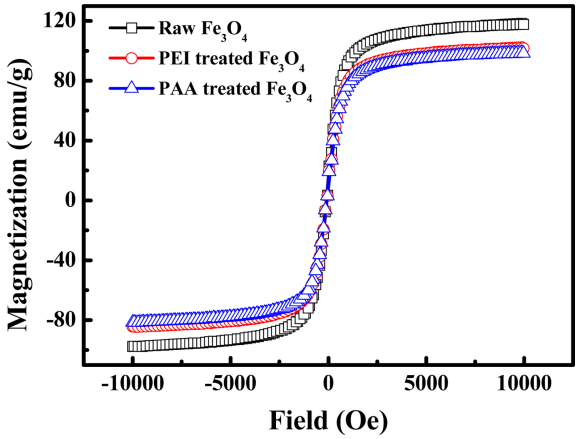

Fig. 4. Hysteresis loop of Fe_3O_4 specimens.

be lost.

The magnetic properties shown in Fig. 4 indicate that the superparamagnetic properties of the raw Fe_3O_4 particles did not change due to the presence of PEI or PAA. The hysteresis loops show that the overall residual magnetization values and coercive force values were low, indicating that the particles may be easily aggregated or re-dispersed by applying or removing an external magnetic field. However, treatment with PEI and PAA changed the saturation magnetization values of the raw Fe_3O_4 particles. The initial saturation magnetization value of 118 emu/g was reduced to 102.3 emu/g for the PEI-treated particles and to 98.9 emu/g for the PAA-treated particles. This may be the result of the decrease of the ratio of the magnetic particles due to the presence of PEI and PAA.[8] The saturation magnetization value of the PAA-treated particles was lower than that of the PEI-treated particles, because the ratio of magnetic particles was lower in the PAA-treated particles due to damage on the particle surface. However, Fig. 4 shows that the saturation magnetization values and the superparamagnetic properties of the samples were still high enough to cause aggregation and re-dispersion, indicating that the magnetic properties of the starting materials were not significantly decreased by the introduction of the external substances.[8,14]

4. Conclusions

The surface of raw Fe_3O_4 particles was treated with PEI and PAA, which are representative polymer compounds having functional groups; the presence of functional groups on the Fe_3O_4 particle surface, as well as the change in the dispersion properties, was investigated. The peaks found in the FT-IR spectra of the samples verified the presence of amine functional groups on the surface of the PEI-treated particles and the presence of carboxyl groups on the surface of the PAA-treated particles. The electrostatic repulsive force that these functional groups have decreased the mean particle size and the polydispersity index of the particles. The dispersion was more uniform in the PAA-treated particles. The shapes of the particles partially changed after surface treatment using the polymer compounds, resulting even in damage to the PAA-treated particles. However, the change of the magnetic properties due to the loss of some of the nanoparticles was negligible, and thus the magnetic properties of the PAA-treated particles were not significantly different from those of the PEI-treated particles. Therefore, surface treatment of Fe_3O_4 particles with PAA, which may form carboxyl functional groups on the particle surface, may be more useful than surface treatment using PEI for particle dispersion.

REFERENCES

1. L. Li, A. Kovalchuk, H. Fei, Z. Peng, Y. Li, N. D. Kim, C. Xiang, Y. Yang, G. Ruan, and J. M. Tour, "Enhanced Cycling Stability of Lithium-Ion Batteries Using Graphene-Wrapped Fe_3O_4-Graphene Nanoribbons as Anode Materials," *Adv. Energy Mater.*, **5** [14] 1500171 (2015).
2. K. Hayashi, M. Nakamura, W. Sakamoto, T. Yogo, H. Miki, S. Ozaki, M. Abe, T. Matsumoto, and K. Ishimura, "Superparamagnetic Nanoparticle Clusters for Cancer Theranostics Combining Magnetic Resonance Imaging and Hyperthermia Treatment," *Theranostics*, **3** [6] 366-76 (2013).
3. A. Sukhov, L. Chotorlishvili, P. P. Horley, C.-L. Jia, S. K. Mishra, and J. Berakdar, "On the Superparamagnetic Size Limit of Nanoparticles on a Ferroelectric Substrate," *J. Phys. D: Appl. Phys.*, **47** [15] 155302 (2014).
4. M. J. Chen, H. Shen, X. Li, and H. F. Liu, "Facile Synthesis of Oil-Soluble Fe_3O_4 Nanoparticles Based on a Phase Transfer Mechanism," *Appl. Surf. Sci.*, **307** 306-10 (2014).
5. Q. A. Pankhurst, J. Connolly, S. K. Jones, and J. Dobson, "Applications of Magnetic Nanoparticles in Biomedicine," *J. Phys. D: Appl. Phys.*, **36** [13] 167-81 (2003).
6. S. Tenzer, D. Docter, J. Kuharev, A. Musyanovych, V. Fetz, R. Hecht, F. Schlenk, D. Fischer, K. Kiouptsi, C. Reinhardt, K. Landfester, H. Schild, M. Maskos, S. K. Knauer, and R. H. Stauber, "Rapid Formation of Plasma Protein Corona Critically Affects Nanoparticle Pathophysiology," *Nat. Nanotechnol.*, **8** 772-81 (2013).
7. I. Safarik and M. Safarikova, "Magnetic Techniques for the Isolation and Purification of Proteins and Peptides," *Biomagn. Res. Technol.*, **2** [1] 7 (2004).
8. G. S. An, S. W. Choi, D. H. Chae, H. S. Lee, H. J. Kim, Y. J. Kim, Y. G. Jung, and S. C. Choi, "γ-Fe_3O_4@SiO_2 Core-Shell Structured Nanoparticle: Fabrication via Surface Treatment and Application for Plasmid DNA Purification," *Ceram. Int.*, **43** 12888-92 (2017).
9. S. B. Wee, H. C. Oh, T. G. Kim, G. S. An, and S. C. Choi, "Role of N-methyl-2-pyrrolidone for Preparation of Fe_3O_4@SiO_2 controlled the shell thickness, *J. Nanopart. Res.*, **19** 143 (2017).
10. P. Tancredi, S. Botasini, O. Moscoso-Londoño, E. Méndez, and L. M. Socolovsky, "Polymer-Assisted Size Control of Water-Dispersible Iron Oxide Nanoparticles in Range between 15 and 100 nm," *Colloids Surf., A*, **464** 45-51 (2015).

11. Y. Takeno, Y. Murakami, T. Sato, T. Tanigaki, H. S. Park, D. Shindo, R. M. Ferguson, and K. M. Krishnan, "Morphology and Magnetic Flux Distribution in Superparamagnetic Single-Crystalline Fe_3O_4 Nanoparticle Rings," *Appl. Phys. Lett.*, **105** 183102 (2014).
12. G. S. An, S. W. Choi, T. G. Kim, J. R. Shin, Y. I. Kim, S. C. Choi, and J. G. Jung, "Amino-Functionalization of Colloidal Alumina Particles for Enhancement of the Infiltration Behavior in a Silica-Based Ceramic Core," *Ceram. Int.*, **43** [1] 157-61 (2017).
13. G. S. An, J. S. Han, J. U. Hur, and S. C Choi, "Synthesis of Sub-Micro Sized High Purity Zirconium Diboride Powder through Carbothermal and Borothermal Reduction Method," *Ceram. Int.*, **43** [8] 5896-900 (2017).
14. Y. V. Kolen'ko, M. Bañobre-López, C. Rodríguez-Abreu, E. Carbó-Argibay, A. Sailsman, Y. Piñeiro-Redondo, M. F. Cerqueira, D. Y. Petrovykh, K. Kovnir, O. I. Lebedev, and J. Rivas, "Large-Scale Synthesis of Colloidal Fe_3O_4 Nanoparticles Exhibiting High Heating Efficiency in Magnetic Hyperthermia," *J. Phys. Chem. A*, **118** [16] 8691-701 (2014).